Spin-Orbital Excitations in Ca_2RuO_4 Revealed by Resonant Inelastic X-Ray Scattering

L. Das,[1] F. Forte,[2,3] R. Fittipaldi,[2,3] C. G. Fatuzzo,[4,‡] V. Granata,[2,3] O. Ivashko,[1] M. Horio,[1] F. Schindler,[1] M. Dantz,[5] Yi Tseng,[5] D. E. McNally,[5] H. M. Rønnow,[4] W. Wan,[6] N. B. Christensen,[6] J. Pelliciari,[5,*] P. Olalde-Velasco,[5,†] N. Kikugawa,[7,8] T. Neupert,[1] A. Vecchione,[2,3] T. Schmitt,[5] M. Cuoco,[2,3] and J. Chang[1]

[1]*Physik-Institut, Universität Zürich, Winterthurerstrasse 190, CH-8057 Zürich, Switzerland*
[2]*CNR-SPIN, I-84084 Fisciano, Salerno, Italy*
[3]*Dipartimento di Fisica "E.R. Caianiello," Università di Salerno, I-84084 Fisciano, Salerno, Italy*
[4]*Institute of Physics, École Polytechnique Fedérale de Lausanne (EPFL), CH-1015 Lausanne, Switzerland*
[5]*Swiss Light Source, Paul Scherrer Institut, CH-5232 Villigen PSI, Switzerland*
[6]*Department of Physics, Technical University of Denmark, DK-2800 Kongens Lyngby, Denmark*
[7]*National Institute for Materials Science, 1-2-1 Sengen, Tsukuba, 305-0047 Japan*
[8]*National High Magnetic Field Laboratory, Tallahassee, Florida 32310, USA*

(Received 4 July 2017; revised manuscript received 28 January 2018; published 22 March 2018)

The strongly correlated insulator Ca_2RuO_4 is considered as a paradigmatic realization of both spin-orbital physics and a band-Mott insulating phase, characterized by orbitally selective coexistence of a band and a Mott gap. We present a high resolution oxygen K-edge resonant inelastic x-ray scattering study of the antiferromagnetic Mott insulating state of Ca_2RuO_4. A set of low-energy (about 80 and 400 meV) and high-energy (about 1.3 and 2.2 eV) excitations are reported, which show strong incident light polarization dependence. Our results strongly support a spin-orbit coupled band-Mott scenario and explore in detail the nature of its exotic excitations. Guided by theoretical modeling, we interpret the low-energy excitations as a result of composite spin-orbital excitations. Their nature unveils the intricate interplay of crystal-field splitting and spin-orbit coupling in the band-Mott scenario. The high-energy excitations correspond to intra-atomic singlet-triplet transitions at an energy scale set by Hund's coupling. Our findings give a unifying picture of the spin and orbital excitations in the band-Mott insulator Ca_2RuO_4.

DOI: 10.1103/PhysRevX.8.011048

Subject Areas: Condensed Matter Physics, Materials Science, Strongly Correlated Materials

I. INTRODUCTION

Spin-orbit coupling (SOC) is a central thread in the search for novel quantum material physics [1]. A particularly promising avenue is the combination of SOC and strong electron correlations in multi-orbital systems. This scenario is realized in heavy transition metal oxides composed of 4*d* and 5*d* elements. Iridium oxides (iridates) such as Sr_2IrO_4 are prime examples of systems where SOC plays a defining role in shaping the Mott insulating ground state [2]. In fact, spin-orbit entanglement essentially outplays the effectiveness of the usually influential crystal field δ. Of equal interest is the complex regime where SOC and crystal-field energy scales are comparable. Here, Ca_2RuO_4 is a topical material that displays a wealth of physical properties. A record-high nonsuperconducting diamagnetic response has, for example, been reported recently [3]. Superconductivity emerges in strained films [4] or upon application of hydrostatic pressure to bulk crystals [5]. Neutron and Raman scattering experiments have demonstrated both phase and amplitude spin-excitation modes consistent with the existence of a spin-orbit exciton [6–8]. Moreover, measurements of the paramagnetic insulating band structure [9] were interpreted in favor of an orbitally differentiated band-Mott insulating ground state [10,11]. This rich phenomenology of Ca_2RuO_4 is a manifestation of the interplay between multiple energy scales—specifically, the Coulomb interaction U, Hund's coupling J_H, the crystal-field splitting δ, and SOC λ. In particular, a

*Present address: Department of Physics, Massachusetts Institute of Technology, Cambridge, MA 02139, USA.
†Present address: Instituto de Fisica, Benemerita Universidad Autonoma de Puebla, Apdo. Postal J-48, Puebla, Puebla 72570, Mexico.
‡Present address: Materials Sciences Division, Lawrence Berkeley National Lab, 1 Cyclotron Road, Berkeley, CA 94720, USA.

tendency towards an orbital selective Mott state is expected to be driven by Hund's coupling [12]. Furthermore, the band-Mott scenario is triggered by a crystal field that renders the d_{xy} orbital band insulating, such that the resulting half-filled d_{xz}, d_{yz} band undergoes a conventional Mott transition driven by the Coulomb interaction [11].

The low-energy electronic excitations of Ca_2RuO_4 have been interpreted within an exciton picture where SOC enters as an important parameter [13]. A similar framework has been applied to layered iridates—with a 5/6-filled t_{2g} shell—where a $J_{\text{eff}} = 1/2$ quasiparticle emerges from strong SOC. The existence of this quasiparticle has been confirmed by detailed resonant inelastic x-ray scattering (RIXS) studies of both spin and orbital excitations [14,15]. For Ca_2RuO_4, with modest spin-orbit coupling strength, studies of the spin excitations have been interpreted as evidence for a similar composite $J_{\text{eff}} = 1$ quasiparticle [16,17]. However, the full manifold of the low-lying spin-orbital excitations of Ca_2RuO_4 has not yet been observed. The possibility to detect Ru d-orbital excitations through the oxygen K edge [18,19] offers a unique opportunity in the case of ruthenates, where direct L-edge RIXS is not yet available for high-resolution measurements. Moreover, spin-orbital excitations are mostly inaccessible to neutron scattering.

Here, we present an oxygen K-edge RIXS study of Ca_2RuO_4 focusing on the magnetically ordered phase. Two low-energy excitations (80 and 400 meV) and two high-energy excitations (1.3 and 2.2 eV) are identified. Light-polarization analysis yields insight to the internal orbital character of these excitations. A detailed analysis of the 400-meV excitation uncovered a weak dispersion, consistent with a propagating nature.

In contrast, the high-energy excitations are closely linked to Hund's coupling energy scale J_H. The excitations reported here on Ca_2RuO_4 are unique features of (1) a band-Mott insulating phase controlled by Hund's coupling and Coulomb interactions, and (2) a composite spin-orbital excitation resulting from SOC. Hence, our results give experimental support for Ca_2RuO_4 being in a spin-orbit-coupled band-Mott insulating phase. Thus, it provides an experimental unification of the band-Mott [9,11] and van Vleck-type Mott [16,20] insulator scenarios.

II. METHODS

High-quality single crystals of Ca_2RuO_4 were grown using the floating zone techniques [21,22]. X-ray absorption spectroscopy (XAS) and RIXS [23] were carried out at the ADRESS beamline [24,25] at the Swiss Light Source (SLS). The scattering geometry is indicated in Fig. 1(a). A fixed angle of 130° between incident light and scattered light was used. In-plane momentum is varied by controlling the incident photon angle θ shown in Fig. 1(a). Grazing and normal incidence conditions refers to $\theta \approx 90°$ and 0°, respectively. Linear vertical (LV) and horizontal (LH) light polarizations were used to probe the oxygen K edge at which an energy resolution of 29 meV or better (half width

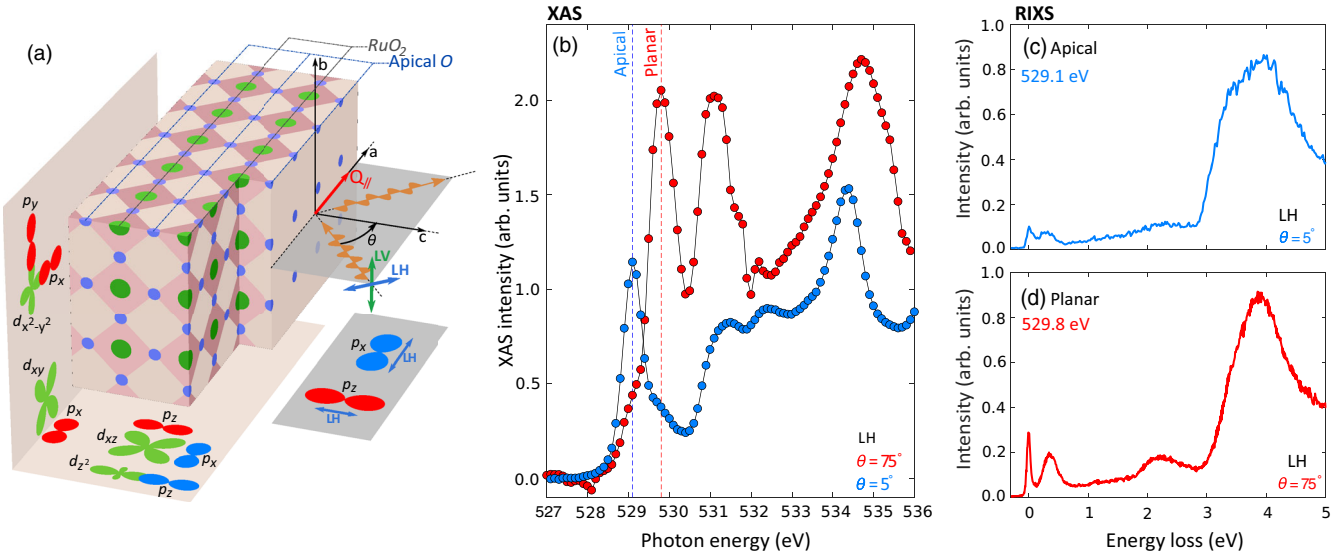

FIG. 1. (a) RIXS geometry with respect to the crystal lattice of Ca_2RuO_4 is displayed schematically. Ruthenium and oxygen sites are shown with filled green and blue circles, respectively. The variable incident angle θ is defined with respect to the RuO_2 and apical oxygen planes. Using LV and LH polarized light, for different θ, sensitivity to either oxygen p_x, p_y, or p_z orbitals can be obtained. These oxygen orbitals in turn hybridize with different unoccupied t_{2g} and e_g states on the ruthenium site. (b–d) XAS and RIXS spectra recorded with linear horizontal light for near grazing and normal incident light conditions as indicated. (b) Background-subtracted x-ray absorption spectra recorded with settings that optimize either the apical or planar oxygen K-edge resonances as indicated by the dashed vertical lines. Panels (c) and (d) display RIXS spectra measured at the planar and apical oxygen K edges.

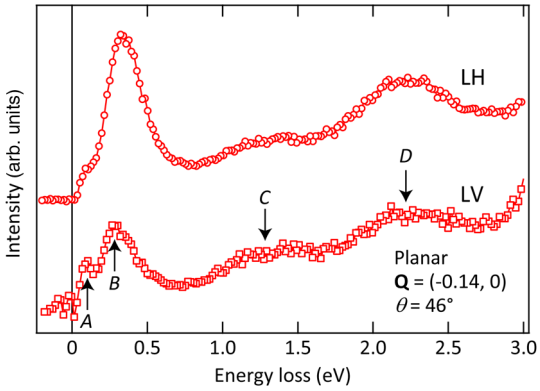

FIG. 2. Planar RIXS spectra, with elastic scattering subtracted and recorded with LH and LV light polarization for incident angle (momentum transfer) as indicated. Vertical arrows indicate the four excitations labeled A, B, C, and D. For clarity, the spectra are given an arbitrary vertical shift.

at half maximum) was obtained. Despite the orthorhombic low-temperature (S-Pbca) crystal structure of Ca_2RuO_4, we indicate momenta $Q = (h, k, \ell)$ using tetragonal notation in reciprocal lattice units, with $a \approx b = 3.84$ Å and $c \approx 11.95$ Å. Furthermore, since Ca_2RuO_4 is a quasi-two-dimensional system, we consider only the planar component $Q_{||} = (h, k)$ involved in the RIXS process. Throughout this work, elastic scattering is modeled by using a Voigt line shape, allowing subtraction of this component. The presented data are collected at $T = 16$ K unless otherwise indicated.

III. RESULTS

XAS spectra recorded with LH light polarization near normal and grazing incidence conditions are shown in Fig. 1(b). Good agreement with previous published XAS experiments [26–28] is found when overlap in temperature, light polarization, and incident angle allows for a comparison. As is common in single-layer perovskite structured transition metal oxide materials [26,27,29,30], the planar oxygen absorption resonance is found to be 1–2 eV above that of the apical site. As previously reported [26,27,31], the apical and planar oxygen K-edge peaks are found at about 529.1 eV and 529.8 eV [see Fig. 1(b)]. These resonances stem from hybridization of the oxygen p-bands with the ruthenium t_{2g} states, whereas the resonances at higher photon energies are related to hybridization with unoccupied e_g states.

In Fig. 2, four RIXS distinct excitations—labeled A, B, C, and D—with approximate energy losses of 0.08, 0.4, 1.3, and 2.4 eV, are displayed in addition to elastic scattering and dd excitations in the 3–5-eV range [see Figs. 1(c) and 1(d)]. Only the B excitation (at about 0.4 eV) has previously been discussed in Ref. [31]. The amplitudes of these excitations strongly depend on incident light angle and polarization.

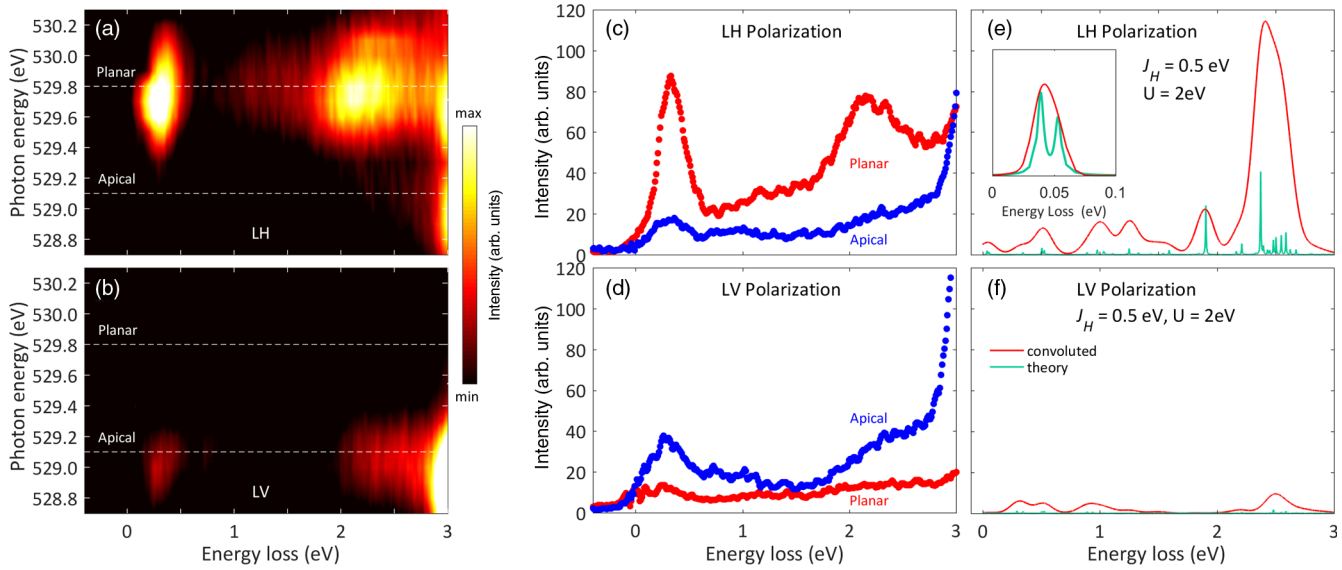

FIG. 3. Polarization dependence of the RIXS spectra versus incident photon energy. (a,b) RIXS response, in false intensity scale, as a function of energy loss and incident photon energy of LH and LV light polarization for the grazing incidence condition, as indicated. Horizontal dashed lines show the positions of the apical and planar resonances obtained from XAS. (c,d) RIXS spectra, with the elastic response subtracted, at the apical (blue lines) and planar (red lines) oxygen resonances for the respective light polarizations. (e,f) Calculated RIXS spectra for the planar site with respect to linear horizontal (c) and vertical (d) light polarization (see text for a detailed explanation of the model). Green lines indicate the expected excitations, and the solid red line is obtained by Gaussian convolution to mimic instrumental resolution. A standard deviation of $\sigma = 70$ meV was applied in panels (e) and (f), whereas $\sigma = 7$ meV was used for the inset, which displays a zoom on the lowest excitations at around 40 meV.

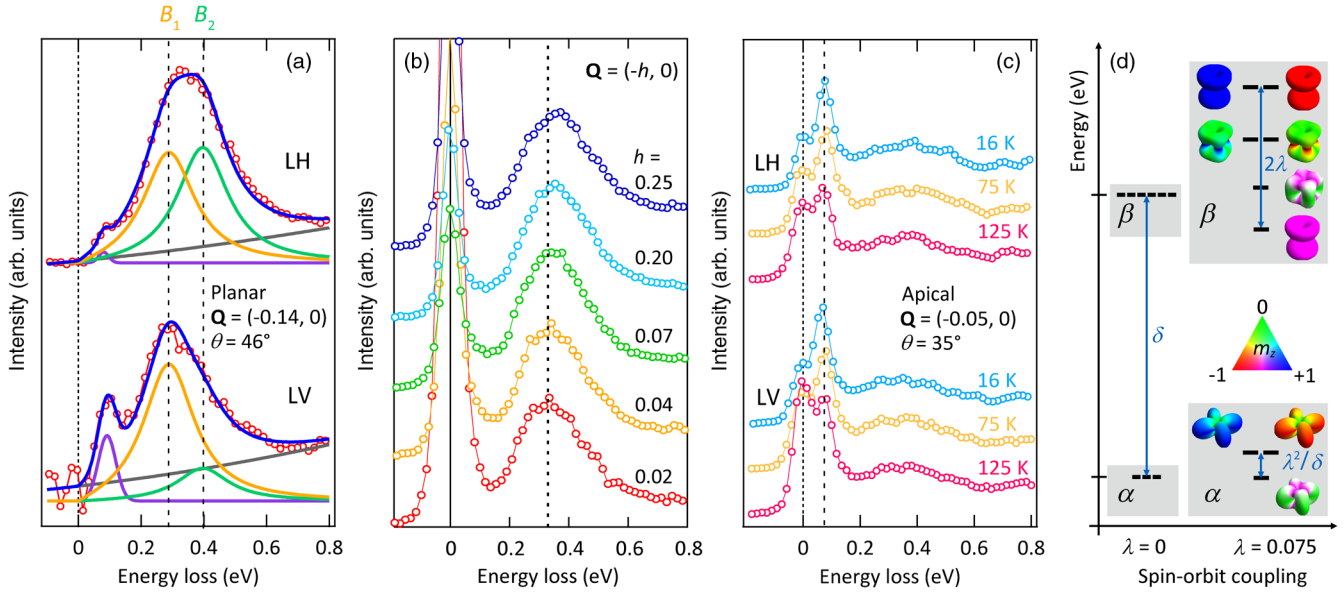

FIG. 4. (a) Same spectra as in Fig. 2 displayed with emphasis on the low-energy excitations. Solid blue lines are a four-component fit, including a smoothly growing background (gray lines—second-order polynomial form), the 80-meV excitation (purple line—Gaussian line shape), and two modes with damped harmonic oscillator line shape [32–34] labeled B_1 (yellow) and B_2 (green) for the excitation at 400 meV. The position and width of B_1 and B_2 are assumed to be identical for LV and LH polarization. Peak amplitudes, by contrast, are left as open fit parameters irrespectively of light polarization. (b) RIXS spectra at planar resonance recorded using linear horizontal light polarization as a function in-plane momenta, as indicated. (c) Apical RIXS spectra recorded with LV and LH polarization near normal incidence for temperatures, as indicated. Lines in panels (b) and (c) are guides to the eye. (d) Schematics of low-lying energy levels of an interacting model for a single ruthenium site for spin-orbit coupling λ set to zero (left) and to the physical value in Ca_2RuO_4 (right). With four electrons, one of the orbitals d_{xy}, d_{xz}, d_{yz} is doubly occupied, and the two singly occupied electrons are in a spin-triplet state. Finite spin-orbit coupling lifts the degeneracies of the two sectors denoted α and β. The character of the doubly occupied orbital is displayed along with a color scale indicating the directional dependence of the total spin m_z moment.

These matrix elements are furthermore different on the apical and planar resonances. All four excitations are therefore not necessarily visible in a single spectrum—as in Fig. 2. We start by discussing the two most intense excitations, B and D. Plotting the photon-energy-dependent RIXS response (Fig. 3) for the grazing incident condition, these two excitations are the most prominent features in the spectra. They are particularly intense on the planar oxygen K-edge resonance for LH polarization. Interestingly, these excitations are virtually "turned off" when the light polarization is switched to LV polarization. The opposite polarization dependence is observed on the apical site, where the excitations are observed for LV and suppressed for LH polarized light. The same light polarization analysis for an incident angle between grazing and normal incidence is shown in Figs. 2 and 4(a) for the planar resonance. It reveals several important insights. (1) The line shape of the B excitation is strongly dependent on the incident light polarization. In fact, the peak maximum depends on light polarization [Fig. 4(a)]. (2) The D excitation is stronger for the grazing incidence and generally weaker in the LV channel. By contrast, the C excitation is more visible with LV polarization (Fig. 2). (3) The same is true for the A excitation: On the planar resonance, it is barely resolvable with LH light, but it appears clearly in the LV channel. In Fig. 4(c), we demonstrate how the A excitation appears in both the LH and LV channels on the apical resonance (near normal incidence). (4) The linewidth of the A excitation is essentially resolution limited and hence much sharper than that of B. The implications of this observation will be discussed in greater detail below.

We now discuss temperature and momentum dependence of the A and B excitations. As evident from Fig. 4(c), both the A and B excitations persist into the paramagnetic phase. The momentum dependence—along the $(h, 0)$ (Ru—O bond) direction—of planar spectra recorded with LH polarization is shown in Fig. 4(b). The peak maximum position, extracted from fitting the derivative of the spectra, reveals a weak momentum dependence, consistent with a dispersive B sector. The extracted momentum dispersion of the excitation is reported [Fig. 5(b)] with a minimum at the zone center. In comparison, no dispersion of the A excitation could be resolved within the applied energy resolution. For completeness, the RIXS data are compared with the amplitude spin excitation mode reported by inelastic neutron scattering (INS) [7].

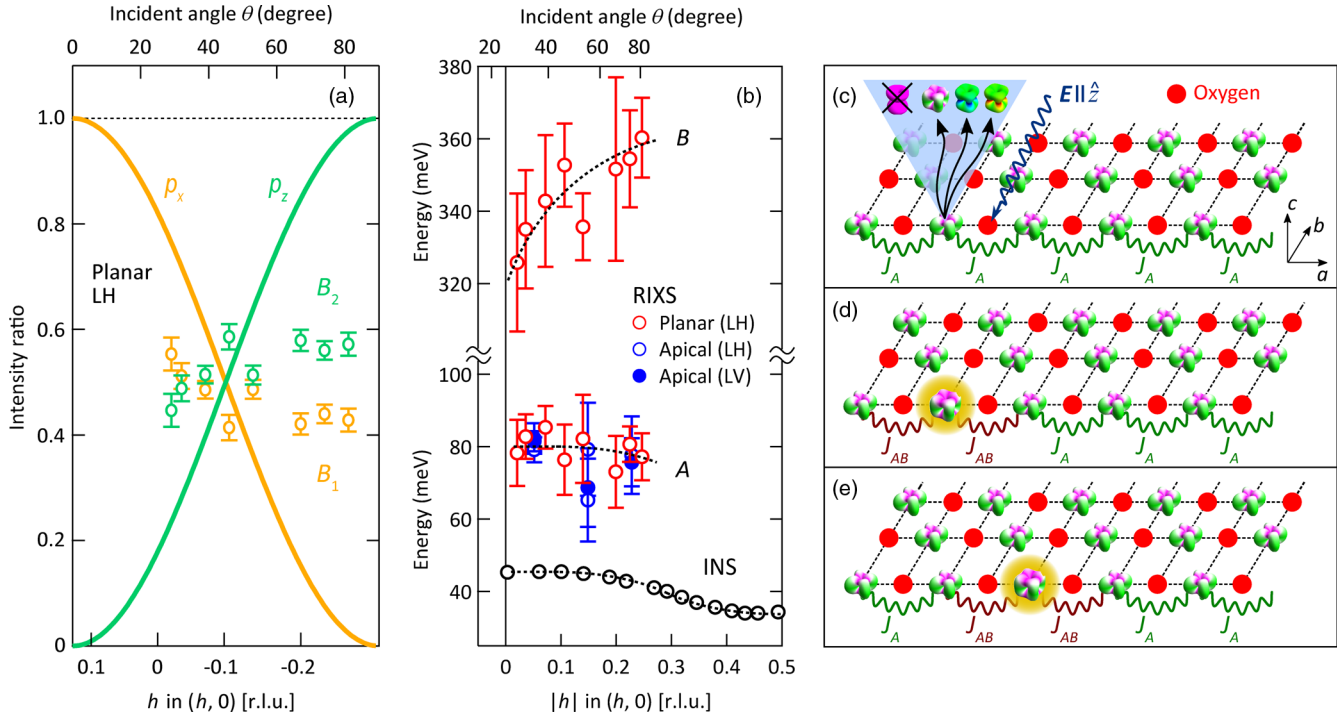

FIG. 5. Momentum-dependent analysis of the low-energy excitations. (a) Peak amplitudes of the assumed B_1 (yellow) and B_2 (green) modes extracted from fits (with fixed peak widths and positions—see text) as shown in Fig. 4(a). Corresponding solid cosine squared lines indicate, for LH, the expected coupling to the p_x and p_z oxygen orbitals. (b) Extracted dispersion along the $Q = (h, 0)$ direction of the A and B excitations in meV, as shown before in panel (a) of Fig. 4. The dispersion is defined by the peak maxima, which in the case of the B excitation, is derived from a derivative of the spectra. Error bars indicate standard deviations 3σ and σ for the A and B, respectively. Comparison to the spin excitation branch observed by neutron scattering (reproduced from Ref. [7]) along the same direction is also shown in panel (b). Dashed lines are guides to the eye. (c) Schematic of an oxygen K-edge RIXS process creating a local excitation between the α and β sectors (see Fig. 4). Panels (d) and (e) illustrate propagation of the spin-orbital excitation. The nearest-neighbor couplings are denoted J_A between sites in the α sector and J_{AB} between α and β sectors.

IV. DISCUSSION

The exact nature of the Mott insulating state of Ca_2RuO_4 has long been debated. Different theoretical models have been put forward [10,11,35–37]. Some of them suggest that all t_{2g} orbitals are involved in the Mott transition. Other models propose that crystal fields drive the d_{xy} states band insulating, and the Mott physics is induced on the resulting half-filled $d_{xz/yz}$ bands [10]. A recent ARPES study of the paramagnetic Mott insulating state supports this combined band-Mott insulating scenario [9]. This conclusion was reached by visual comparison of the measured and calculated spectral functions for different scenarios.

Based on this development, it is interesting to evaluate the implications of the band-Mott scenario on the XAS and RIXS spectra. When the d_{xy} orbital is (almost) completely occupied, it is inaccessible to the XAS processes that require unoccupied states. Therefore, d_{xz} and d_{yz} are the main active t_{2g} states available for absorption. The XAS spectra, shown in Fig. 1(b), are in perfect accordance with this picture. For example, near the grazing incident condition using LH polarization, the core electron is promoted to the p_z oxygen orbital that, at the planar site, hybridizes with $d_{xz/yz}$. Indeed, a pronounced response is observed at the planar oxygen K-edge resonance, whereas the intensity at the apical resonance is strongly suppressed. Further, changing to normal incidence (keeping LH polarization), the core electrons are promoted to the oxygen p_x orbital, which at the planar site, hybridizes with d_{xy} and at the apical site with d_{xz}. As shown in Fig. 1, the XAS response flips to the apical resonance. Our XAS results thus suggest that the unoccupied t_{2g} states have predominant $d_{xz/yz}$ character.

The intensities of the RIXS spectra naturally follow the polarization dependence of the XAS response. We notice that the two excitations B and D observed at 0.4 eV and 2.2 eV, respectively, are most pronounced near grazing incidence with LH polarization at the planar oxygen resonance. This is exactly where the oxygen hybridization with $d_{xz/yz}$ is optimized. We thus conclude that the excitations are intimately linked to the unoccupied $d_{xz/yz}$ states. The A excitation, by contrast, is observed on both the apical and planar resonances with both LH and LV polarization. This suggests that the orbital character of this excitation involves a mixture of d_{xy} and $d_{xz/yz}$ states.

To connect our data with a microscopic physical picture, we computed the RIXS response for an interacting model

of Ca_2RuO_4. Within the fast collision approximation [23,38], the RIXS cross section for exciting an electron from the oxygen $1s$ level into a $2p_k$ level, with $k = x, y, z$, is given by

$$I_{p_k}^{\mathrm{p/a}} \propto \sum_m \sum_i |\langle m|\hat{n}_{p_k,i}^{\mathrm{p/a}}|0\rangle|^2 \delta[\omega - (E_m - E_0)], \quad (1)$$

where the operator $\hat{n}_{p_k,i}^{\mathrm{p/a}}$ measures the *hole* density of oxygen p_k orbitals on all planar (p) or apical (a) oxygen sites surrounding the ruthenium site i, $|0\rangle$ is the ground state with energy E_0, and the sum m runs over all excited states $|m\rangle$ with energies E_m.

To discuss the spectra presented in Figs. 1 and 3, we model a cluster of two ruthenium sites connected by one planar oxygen site (see Ref. [39]). The ruthenium-site Hamiltonian consists of three terms: (1) crystal-field splitting δ between the d_{xy}, d_{xz}, d_{yz} orbitals, (2) SOC λ, and (3) the Coulomb interaction, which is expanded into intraorbital and interorbital Hubbard interactions of strengths U and $(U - 5J_H/2)$, respectively. Interorbital Hund's coupling and the pair-hopping term are both of strength J_H. To evaluate the model, material-specific values $\delta = 0.3$ eV, $\lambda = 0.075$ eV, $U = 2$ eV, and $J_H = 0.5$ eV [27,31,40] are used. Similar values of δ, U, and J_H have been used for DMFT calculations [9] of Ca_2RuO_4, and the ratio $\delta/(2\lambda) = 2$ is comparable to what was used in modeling the spin-excitation dispersion observed by neutron scattering [7]. We stress that, qualitatively, the model is not very sensitive to the exact set of parameters. Although the ratio of spectral weight between the low- and high-energy excitations for horizontal polarization is different from the data, our results presented in Figs. 3(e) and 3(f) qualitatively reproduce the experimental spectra, in particular, the excitation at about 2.2 eV as well as the polarization dependence of the spectral weight. We point out that the spectral features at about 1 eV and 2 eV arise from single and double singlet-triplet excitations at the ruthenium site with an energy of $2J_H$ and $4J_H$, respectively. Thus, this provides an explanation for the observed C and D excitations. Such modes are spin-orbit activated when mixing d^4 with d^3 or d^5 states, and they represent the lowest-energy singlet-triplet excitations when the total number of doubly occupied orbitals at the ruthenium sites is held fixed (see Ref. [39]).

To elucidate the nature of the low-energy excitations, we concentrate on the local electronic structure at a single ruthenium site. The low-energy configurations have four electrons (d^4), one doubly occupied orbital (doublon), and the two other electrons in a spin-triplet state. For $\lambda = 0$, the model has a threefold-degenerate ground-state manifold α with a doublon in the d_{xy} orbital. The lowest-lying excitation sector β is sixfold degenerate at energy $E_{\alpha\beta} = \delta$, with the doublon in the d_{xz} and d_{yz} orbitals [see Fig. 4(d)]. Finite spin-orbit coupling has two effects: (i) It lifts the degeneracies of the α and β states by introducing a splitting of about λ^2/δ and 2λ, respectively, and, crucially, (ii) it mixes the orbital character of the doublon state. The β states thus correspond to a spin-orbital excitation. The splitting of α states gives rise to low-energy excitations that have been studied using neutron scattering [7] [reproduced in Fig. 4(b)]. Just as the β sector has an expected internal orbital structure, it was recently demonstrated by Raman spectroscopy that the low-energy α sector also consists of multiple excitations. In fact, a Raman study also revealed two excitations around 80 meV and associated them with two-Higgs and two-magnon scattering modes [8]. Although optical 80–100 meV phonon modes are not uncommon in transition metal oxides, the Raman study [8] suggests that our A excitation is of magnetic origin. To this end, we stress that our model spectra shown in Fig. 3(e) display low-energy modes with maximum intensity at about 40 meV. It can be assigned to the amplitude and phase excitations arising from the effective $J_{\mathrm{eff}} = 1$ configurations in the α sector. Our cluster analysis, by construction, does not allow us to obtain multiple amplitude excitations associated with the interacting $J_{\mathrm{eff}} = 1$. However, a two-scattering mode (i.e., near 80 meV) is, in principle, expected and would emerge in a larger cluster calculation, eventually considering the RIXS cross section at the oxygen K edge beyond the fast collision approximation. The predicted 40-meV magnetic mode, observed by neutron scattering, should, in principle, also enter into the RIXS cross section. However, it is not observed in our experiment because of the finite energy resolution.

The broadness of the B excitation and its light polarization dependence may be interpreted as a consequence of the internal structure of the β sector. In fact, it is possible to fit the B excitation with two internal levels labeled B_1 and B_2. Keeping identical linewidths and fixed peak positions, the fits describe both the light polarization dependence [Fig. 4(a)] and the momentum dependence by fitting the peak amplitudes. In particular, the observed light polarization dependence for a fixed incident angle (momentum transfer) strongly suggests that the B excitation indeed has an internal orbital structure. This structure constitutes a clear difference from the single-exciton excitation found on the strongly spin-orbit coupled Mott insulator Sr_2IrO_4 [15].

The internal structure raises the need to clarify whether the observed dispersion of the B excitation is a result of matrix element variation of this internal structure. By varying the incident angle (momentum transfer) with LH polarization, a switch between p_z (grazing incidence) and p_x (normal incidence) is effectuated. The expected sensitivity to the p_z and p_x oxygen orbitals is shown in Fig. 5(a). In the same figure, the fitted peak amplitudes of the B_1 and B_2 levels are shown. As they vary only weakly with momentum, the matrix element effect does not provide a plausible explanation for the observed dispersion. We thus conclude that the dispersion is intrinsic, which in turn indicates the itinerant nature of this sector.

When charge hopping between ruthenium sites is reinstated, these local spin-orbit excitons can propagate. Indeed, they acquire a dispersion through virtual processes involving d^3-d^5 excitations on neighboring ruthenium sites. Within second-order perturbation theory, one obtains an estimate of the bandwidth of the spin-orbital excitation in the range of about 30–40 meV, using $t \sim 0.25$–0.3 eV [11] for the ruthenium intersite hopping and $\delta = 0.28$ eV, $\lambda = 0.075$ eV, $U = 2.2$ eV, and $J_H = 0.4$ eV for the other electronic parameters (see Ref. [39]). It is furthermore expected that excitations in the α sector exhibit a weaker dispersion due to the smaller exchange amplitude between the $J_{\text{eff}} = 1$ modes. Our model thus qualitatively account for the fact that the B excitation disperses about 30 meV over half a zone, whereas the A excitation, according to inelastic neutron scattering [7] [see Fig. 5(b)], disperses no more than 20 meV over the entire zone.

V. CONCLUSIONS AND OUTLOOK

In summary, we have carried out a comprehensive oxygen K-edge RIXS study of Ca_2RuO_4. We demonstrate that the strong light polarization dependence of the signal is a direct manifestation of the band-Mott insulating nature of Ca_2RuO_4. The hybridization between oxygen p and ruthenium d states thus primarily involves the $d_{xz/yz}$ orbitals. Although the system has a modest SOC, it is a crucial element to explain our observations. Most importantly, it allows for a distinct set of propagating low-energy (0.4 eV) excitations with a spin-orbital character. The spin-orbit coupling is also relevant for activating the high-energy (about 2.2 eV) nondispersive excitations by the RIXS process, achieved by local conversion of triplet into singlet states. For realistic values of crystal fields, Hund's coupling J_H, Coulomb interaction U, and SOC, all salient features of the RIXS spectra were captured with minimal theoretical modeling. Our results demonstrate that Ca_2RuO_4 is a Mott insulator with a paradigmatic competition between SOC and crystal-field energy scales. Combining RIXS data and theoretical modeling, we unveiled how spin-orbital entangled excitations manifest within a spin-orbit-coupled band-Mott insulator. For future studies, it would be of great interest to further resolve the internal structure of the low-energy excitations. We envision two different pillars of experimental strategies that alone or in combination would allow further insight. (1) As synchrotrons are being upgraded for diffraction limited experiments, flux and resolution at the oxygen K edge will improve. In particular, enhanced energy resolution, in combination with the light polarization analysis put forward here, would allow us to study important information on different orbital characters of these excitations. With gains in energy resolution, the RIXS technique will enter further into the spin-excitation sector. (2) Direct high-resolution RIXS experiments on the ruthenium L edge are another promising avenue.

ACKNOWLEDGMENTS

This work was performed at the ADRESS beamline of the SLS at the Paul Scherrer Institut, Villigen PSI, Switzerland. We thank the ADRESS beamline staff for technical support. L. D., J. C., M. H., O. I., M. D., P. O. V., D. E. M., Y. T, H. M. R and F. S. acknowledge support from the Swiss National Science Foundation through the SINERGIA network Mott Physics beyond the Heisenberg Model, NCCR MARVEL and Grants SNSF DACH, No. BSSGI0-155873, No. 200021-169061, No. P2FRP2-171824, and No. 200021L-141325. L. D. is partially funded by the Swiss Government. J. C. acknowledges the CNR Short Term Mobility Program for partial financial support. J. P. and T. S. acknowledge financial support through the Dysenos AG by Kabelwerke Brugg AG Holding, Fachhochschule Nordwestschweiz and the Paul Scherrer Institute. J. P. acknowledges financial support from the Swiss National Science Foundation Early Postdoc. Mobility Fellowship Project No. P2FRP-171824. P. O. V. acknowledges financial support from the European Community Seventh Framework Programme (FP7/2007–2013) under Grant Agreement No. 290605 (PSIFELLOW/COFUND) and financial support for the work at Puebla Mexico from SEP (511-6/17-8017) PTC-553 and VIEP-BUAP (OLVP-exc17). W. W. and N. B. C. were supported by the Danish Center for Synchrotron and Neutron Science (DanScatt).

[1] W. Witczak-Krempa, G. Chen, Y. B. Kim, and L. Balents, *Correlated Quantum Phenomena in the Strong Spin-Orbit Regime*, Annu. Rev. Condens. Matter Phys. **5**, 57 (2014).

[2] B. J. Kim, H. Jin, S. J. Moon, J.-Y. Kim, B.-G. Park, C. S. Leem, J. Yu, T. W. Noh, C. Kim, S.-J. Oh, J.-H. Park, V. Durairaj, G. Cao, and E. Rotenberg, *Novel $J_{\text{eff}} = 1/2$ Mott State Induced by Relativistic Spin-Orbit Coupling in Sr_2IrO_4*, Phys. Rev. Lett. **101**, 076402 (2008).

[3] C. Sow, S. Yonezawa, S. Kitamura, T. Oka, K. Kuroki, F. Nakamura, and Y. Maeno, *Current-Induced Strong Diamagnetism in the Mott Insulator Ca_2RuO_4*, Science **358**, 1084 (2017).

[4] H. Nobukane, K. Yanagihara, Y. Kunisada, Y. Ogasawara, K. Nomura, Y. Asano, and S. Tanda, *Observation of Localized High-T_c Superconductivity in a Ca_2RuO_4 Nanofilm Single Crystal*, arXiv:1703.09459.

[5] P. L. Alireza, F. Nakamura, S. K. Goh, Y. Maeno, S. Nakatsuji, Y. T. C. Ko, M. Sutherland, S. Julian, and G. G. Lonzarich, *Evidence of Superconductivity on the Border of Quasi-2D Ferromagnetism in Ca_2RuO_4 at High Pressure*, J. Phys. Condens. Matter **22**, 052202 (2010).

[6] S. Kunkemöller, D. Khomskii, P. Steffens, A. Piovano, A. A. Nugroho, and M. Braden, *Highly Anisotropic Magnon Dispersion in Ca_2RuO_4: Evidence for Strong Spin Orbit Coupling*, Phys. Rev. Lett. **115**, 247201 (2015).

[7] A. Jain, M. Krautloher, J. Porras, G. H. Ryu, D. P. Chen, D. L. Abernathy, J. T. Park, A. Ivanov, J. Chaloupka,

G. Khaliullin *et al.*, *Higgs Mode and Its Decay in a Two-Dimensional Antiferromagnet*, Nat. Phys. **13**, 633 (2017).

[8] S.-M. Souliou, J. Chaloupka, G. Khaliullin, G. Ryu, A. Jain, B. J. Kim, M. Le Tacon, and B. Keimer, *Raman Scattering from Higgs Mode Oscillations in the Two-Dimensional Antiferromagnet* Ca_2RuO_4, Phys. Rev. Lett. **119**, 067201 (2017).

[9] D. Sutter, C. G. Fatuzzo, S. Moser, M. Kim, R. Fittipaldi, A. Vecchione, V. Granata, Y. Sassa, F. Cossalter, G. Gatti, M. Grioni, H. M. Ronnow, N. C. Plumb, C. E. Matt, M. Shi, M. Hoesch, T. K. Kim, T. R. Chang, H. T. Jeng, C. Jozwiak, A. Bostwick, E. Rotenberg, A. Georges, T. Neupert, and J. Chang, *Hallmarks of Hund's Coupling in the Mott Insulator* Ca_2RuO_4, Nat. Commun. **8**, 15176 (2017).

[10] A. Liebsch and H. Ishida, *Subband Filling and Mott Transition in* $Ca_{2-x}Sr_xRuO_4$, Phys. Rev. Lett. **98**, 216403 (2007).

[11] E. Gorelov, M. Karolak, T. O. Wehling, F. Lechermann, A. I. Lichtenstein, and E. Pavarini, *Nature of the Mott Transition in* Ca_2RuO_4, Phys. Rev. Lett. **104**, 226401 (2010).

[12] A. Georges, L. de' Medici, and J. Mravlje, *Strong Correlations from Hund's Coupling*, Annu. Rev. Condens. Matter Phys. **4**, 137 (2013).

[13] B. J. Kim and G. Khaliullin, *Resonant Inelastic X-ray Scattering Operators for* t_{2g} *Orbital Systems*, Phys. Rev. B **96**, 085108 (2017).

[14] J. Kim, D. Casa, M. H. Upton, T. Gog, Y.-J. Kim, J. F. Mitchell, M. van Veenendaal, M. Daghofer, J. van den Brink, G. Khaliullin, and B. J. Kim, *Magnetic Excitation Spectra of* Sr_2IrO_4 *Probed by Resonant Inelastic X-ray Scattering: Establishing Links to Cuprate Superconductors*, Phys. Rev. Lett. **108**, 177003 (2012).

[15] J. Kim, M. Daghofer, A. H. Said, T. Gog, J. van den Brink, G. Khaliullin, and B. J. Kim, *Excitonic Quasiparticles in a Spin–Orbit Mott Insulator*, Nat. Commun. **5**, 4453 (2014).

[16] G. Khaliullin, *Excitonic Magnetism in van Vleck-type* d^4 *Mott Insulators*, Phys. Rev. Lett. **111**, 197201 (2013).

[17] A. Akbari and G. Khaliullin, *Magnetic Excitations in a Spin-Orbit-Coupled* d^4 *Mott Insulator on the Square Lattice*, Phys. Rev. B **90**, 035137 (2014).

[18] V. Bisogni, L. Simonelli, L. J. P. Ament, F. Forte, M. Moretti Sala, M. Minola, S. Huotari, J. van den Brink, G. Ghiringhelli, N. B. Brookes, and L. Braicovich, *Bimagnon Studies in Cuprates with Resonant Inelastic X-ray Scattering at the O K Edge. I. Assessment on* La_2CuO_4 *and Comparison with the Excitation at Cu* L_3 *and Cu k Edges*, Phys. Rev. B **85**, 214527 (2012).

[19] X. Lu, P. Olalde-Velasco, Y. Huang, V. Bisogni, J. Pelliciari, S. Fatale, M. Dantz, J. G. Vale, E. C. Hunter, J. Chang, V. N. Strocov, R. S. Perry, M. Grioni, D. F. McMorrow, H. M. Rønnow, and T. Schmitt, *Dispersive Magnetic and Electronic Excitations in Iridate Perovskites Probed by Oxygen K-edge Resonant Inelastic X-ray Scattering*, Phys. Rev. B **97**, 041102 (2018).

[20] A. Akbari and G. Khaliullin, *Magnetic Excitations in a Spin-Orbit-Coupled* d^4 *Mott Insulator on the Square Lattice*, Phys. Rev. B **90**, 035137 (2014).

[21] H. Fukazawa, S. Nakatsuji, and Y. Maeno, *Intrinsic Properties of the Mott Insulator* $Ca_2RuO_{4+\delta}$, Physica (Amsterdam) **281–282B**, 613 (2000).

[22] S. Nakatsuji and Y. Maeno, *Synthesis and Single-Crystal Growth of* $Ca_{2-x}Sr_xRuO_4$, J. Solid State Chem. **156**, 26 (2001).

[23] L. J. P. Ament, M. van Veenendaal, T. P. Devereaux, J. P. Hill, and J. van den Brink, *Resonant Inelastic X-ray Scattering Studies of Elementary Excitations*, Rev. Mod. Phys. **83**, 705 (2011).

[24] V. N. Strocov, T. Schmitt, U. Flechsig, T. Schmidt, A. Imhof, Q. Chen, J. Raabe, R. Betemps, D. Zimoch, J. Krempasky *et al.*, *High-Resolution Soft X-ray Beamline ADRESS at the Swiss Light Source for Resonant Inelastic X-ray Scattering and Angle-Resolved Photoelectron Spectroscopies*, J. Synchrotron Radiat. **17**, 631 (2010).

[25] G. Ghiringhelli, A. Piazzalunga, C. Dallera, G. Trezzi, L. Braicovich, T. Schmitt, V. N. Strocov, R. Betemps, L. Patthey, X. Wang, and M. Grioni, *SAXES, a High Resolution Spectrometer for Resonant X-ray Emission in the 400–1600 eV Energy Range*, Rev. Sci. Instrum. **77**, 113108 (2006).

[26] M. Malvestuto, E. Carleschi, R. Fittipaldi, E. Gorelov, E. Pavarini, M. Cuoco, Y. Maeno, F. Parmigiani, and A. Vecchione, *Electronic Structure Trends in the* $Sr_{n+1}Ru_nO_{3n+1}$ *Family* $(n = 1, 2, 3)$, Phys. Rev. B **83**, 165121 (2011).

[27] T. Mizokawa, L. H. Tjeng, G. A. Sawatzky, G. Ghiringhelli, O. Tjernberg, N. B. Brookes, H. Fukazawa, S. Nakatsuji, and Y. Maeno, *Spin-Orbit Coupling in the Mott Insulator* Ca_2RuO_4, Phys. Rev. Lett. **87**, 077202 (2001).

[28] M. Malvestuto, V. Capogrosso, E. Carleschi, L. Galli, E. Gorelov, E. Pavarini, R. Fittipaldi, F. Forte, M. Cuoco, A. Vecchione *et al.*, *Nature of the Apical and Planar Oxygen Bonds in the* $Sr_{n+1}Ru_nO_{3n+1}$ *Family* $(n = 1, 2, 3)$, Phys. Rev. B **88**, 195143 (2013).

[29] C. T. Chen, F. Sette, Y. Ma, M. S. Hybertsen, E. B. Stechel, W. M. C. Foulkes, M. Schulter, S-W. Cheong, A. S. Cooper, L. W. Rupp, B. Batlogg, Y. L. Soo, Z. H. Ming, A. Krol, and Y. H. Kao, *Electronic States in* $La_{2-x}Sr_xCuO_{4+\delta}$ *Probed by Soft-X-ray Absorption*, Phys. Rev. Lett. **66**, 104 (1991).

[30] M. M. Sala, M. Rossi, S. Boseggia, J. Akimitsu, N. B. Brookes, M. Isobe, M. Minola, H. Okabe, H. M. Rønnow, L. Simonelli, D. F. McMorrow, and G. Monaco, *Orbital Occupancies and the Putative* $j_{\rm eff} = \frac{1}{2}$ *Ground State in* Ba_2IrO_4*: A Combined Oxygen K-edge XAS and RIXS Study*, Phys. Rev. B **89**, 121101 (2014).

[31] C. G. Fatuzzo, M. Dantz, S. Fatale, P. Olalde-Velasco, N. E. Shaik, B. D. Piazza, S. Toth, J. Pelliciari, R. Fittipaldi, A. Vecchione, N. Kikugawa, J. S. Brooks, H. M. Rønnow, M. Grioni, Ch. Rüegg, T. Schmitt, and J. Chang, *Spin-Orbit-Induced Orbital Excitations in* Sr_2RuO_4 *and* Ca_2RuO_4*: A Resonant Inelastic X-ray Scattering Study*, Phys. Rev. B **91**, 155104 (2015).

[32] M. Le Tacon, G. Ghiringhelli, J. Chaloupka, M. M. Sala, V. Hinkov, M. W. Haverkort, M. Minola, M. Bakr, K. J. Zhou, S. Blanco-Canosa *et al.*, *Intense Paramagnon Excitations in a Large Family of High-Temperature Superconductors*, Nat. Phys. **7**, 725 (2011).

[33] C. Monney, T. Schmitt, C. E. Matt, J. Mesot, V. N. Strocov, O. J. Lipscombe, S. M. Hayden, and J. Chang, *Resonant Inelastic X-ray Scattering Study of the Spin and*

Charge Excitations in the Overdoped Superconductor $La_{1.77}Sr_{0.23}CuO_4$, Phys. Rev. B **93**, 075103 (2016).

[34] J. Lamsal and W. Montfrooij, *Extracting Paramagnon Excitations from Resonant Inelastic X-ray Scattering Experiments*, Phys. Rev. B **93**, 214513 (2016).

[35] V. I. Anisimov, I. A. Nekrasov, D. E. Kondakov, T. M. Rice, and M. Sigrist, *Orbital-Selective Mott-Insulator Transition in* $Ca_{2-x}Sr_xRuO_4$, Eur. Phys. J. B **25**, 191 (2002).

[36] M. Cuoco, F. Forte, and C. Noce, *Interplay of Coulomb Interactions and c-axis Octahedra Distortions in Single-Layer Ruthenates*, Phys. Rev. B **74**, 195124 (2006).

[37] M. Cuoco, F. Forte, and C. Noce, *Probing Spin-Orbital-Lattice Correlations in* $4d^4$ *Systems*, Phys. Rev. B **73**, 094428 (2006).

[38] L. J. P. Ament, F. Forte, and J. van den Brink, *Ultrashort Lifetime Expansion for Indirect Resonant Inelastic X-ray Scattering*, Phys. Rev. B **75**, 115118 (2007).

[39] See Supplemental Material at http://link.aps.org/supplemental/10.1103/PhysRevX.8.011048 for a detailed description of our theoretical modelling.

[40] C. N. Veenstra, Z.-H. Zhu, M. Raichle, B. M. Ludbrook, A. Nicolaou, B. Slomski, G. Landolt, S. Kittaka, Y. Maeno, J. H. Dil, I. S. Elfimov, M. W. Haverkort, and A. Damascelli, *Spin-Orbital Entanglement and the Breakdown of Singlets and Triplets in* Sr_2RuO_4 *Revealed by Spin- and Angle-Resolved Photoemission Spectroscopy*, Phys. Rev. Lett. **112**, 127002 (2014).